Sensitivity of intermediate mass fragment flows to the symmetry energy

Z. Kohley, M. Colonna, A. Bonasera, L. W. May, S. Wuenschel, M. Di Toro, S. Galanopoulos, K. Hagel, M. Mehlman, W. B. Smith, G. A. Souliotis, S. N. Soisson, B. C. Stein, R. Tripathi, S. J. Yennello, and M. Zielinska-Pfabe

Phys. Rev. C **85**, 064605 — Published 7 June 2012

DOI: 10.1103/PhysRevC.85.064605

The sensitivity of intermediate mass fragment flows to the symmetry energy

Z. Kohley,[1,2,3,*] M. Colonna,[4] A. Bonasera,[1,4] L. W. May,[1,2] S. Wuenschel,[1,2] M. Di Toro,[4,5] S. Galanopoulos,[1] K. Hagel,[1] M. Mehlman,[1] W. B. Smith,[1] G. A. Souliotis,[1,6] S. N. Soisson,[1,2] B. C. Stein,[1,2] R. Tripathi,[1] S. J. Yennello,[1,2] and M. Zielinska-Pfabe[7]

[1] *Cyclotron Institute, Texas A&M University, College Station, Texas 77843, USA*
[2] *Chemistry Department, Texas A&M University, College Station, Texas 77843, USA*
[3] *National Superconducting Cyclotron Laboratory, Michigan State University, East Lansing, Michigan, 48824, USA*
[4] *Laboratori Nazionali del Sud, INFN, I-95123 Catania, Italy*
[5] *Physics and Astronomy Department, University of Catania, Italy*
[6] *Laboratory of Physical Chemistry, Department of Chemistry, National and Kapodistrian University of Athens, Athens 15771, Greece*
[7] *Smith College, Northampton, MA, USA*

(Dated: May 23, 2012)

The NIMROD-ISiS array was used to study the transverse flow of intermediate mass fragments in 35 MeV/nucleon ^{70}Zn+^{70}Zn, ^{64}Zn+^{64}Zn, and ^{64}Ni+^{64}Ni reactions. The intermediate mass fragment flow was previously shown to be sensitive to the density dependence of the symmetry energy. In order to explore the model dependence of the results, the antisymmetrized molecular dynamics, constrained molecular dynamics, and stochastic mean field models were each compared to the experimental results to extract information on the form of the symmetry energy. The results demonstrate that sensitivity of the models to the nuclear Equation of State can vary significantly based on the treatment of the nuclear dynamics. Despite the differences in the sensitivity, improved agreement with the experimental data is observed for each model with a stiff density dependence of the symmetry energy.

PACS numbers: 25.75.Ld, 25.70.Pq, 25.70.-z,21.65.Ef

I. INTRODUCTION

Constraining the nuclear Equation of State (nEoS) for isospin asymmetric nuclear matter is critical for making accurate predictions and calculations of neutron star properties [1–3]. For example, the radii of neutron stars are related to the pressure of isospin asymmetric nuclear matter, which is proportional to the slope of the symmetry energy [4]. Additionally, the proton fraction as a function of density for a neutron star in β equilibrium has been shown to be very sensitive to the density dependence of the symmetry energy, $E_{sym}(\rho)$ [5, 6]. The proton fraction of the neutron star, and therefore $E_{sym}(\rho)$, defines whether the neutron star will cool quickly through the direct URCA process or more slowly through the standard URCA process.

Heavy-ion collisions (HICs) have begun to provide constraints on the density dependence of the symmetry energy at sub-saturation densities ($\rho < 0.16 fm^{-3}$) [7–14]. However, these constraints are dependent on comparisons with theoretical transport calculations. The effective nucleon-nucleon interaction used in the transport calculation is adjusted to provide different forms of the density dependence of the symmetry energy. Then the transport calculations are compared with the experimental data to determine what form of the effective interaction, or density dependence of the symmetry energy, best reproduces the HIC observable(s). Therefore, the results depend not only on the form of the symmetry energy but also on the treatment of the nuclear dynamics in that specific model [15]. Recent works by Rizzo *et al.* [16] and Colonna *et al.* [17] have demonstrated how the description of the nuclear dynamics in different models can change the multi-fragmentation process and, thus, effect the HIC observables used in constraining the symmetry energy. Similarly, Zhang *et al.* [18] and Coupland *et al.* [19] have explored how adjustments to the input physics of the transport calculations can affect the resulting HIC observables.

For example, examination of experimental π^+/π^- ratios with the mean-field model IBUU04 suggested a soft symmetry energy at high densities [20]. In contrast, a stiff form of the symmetry energy was found to better reproduce the same π^+/π^- data when using the improved isospin dependent quantum molecular dynamics (ImIQMD) model [21]. Similarly, the sensitivity of neutron-to-proton (n/p) ratios to the density dependence of the symmetry was shown to be widely different depending on the choice of the theoretical simulation [11, 22]. It is clear that accurate constraints on the density dependence of the symmetry energy cannot be obtained without consistent theoretical descriptions of the experimental data. Therefore, it is important to compare multiple theoretical calculations to the same HIC observable(s) in order to validate any constraints.

Collective flow has been predicted to be a useful probe for applying constraints on the asymmetric part of the EoS at both high and low densities [7, 8, 10, 23–27]. Recently, we examined the transverse flow of inter-

* zkohley@gmail.com

mediate mass fragments (IMFs) from 35 MeV/nucleon ^{70}Zn+^{70}Zn, ^{64}Zn+^{64}Zn, and ^{64}Ni+^{64}Ni systems [10]. The IMF flow was shown to be sensitive to the density dependence of the symmetry energy through comparison with the antisymmetrized molecular dynamics model [28]. A stiff $E_{sym}(\rho)$ provided the best agreement with the experimental data [10]. In this paper, the sensitivity of the mid-peripheral IMF flow results to $E_{sym}(\rho)$ are further examined through comparison with the antisymmetrized molecular dynamics [28], constrained molecular dynamics [29, 30], and stochastic mean-field [31] models. This provides the opportunity to compare the sensitivity of the IMF flow to the symmetry energy between different theoretical simulations.

II. EXPERIMENTAL SETUP AND ANALYSIS

The Superconducting K500 Cyclotron at the Texas A&M Cyclotron Institute was used to accelerate ^{70}Zn, ^{64}Zn, and ^{64}Ni projectiles to 35 MeV/nucleon, which bombarded ^{70}Zn, ^{64}Zn, and ^{64}Ni self-supporting targets, respectively. The NIMROD-ISiS array (Neutron Ion Multidetector for Reaction Oriented Dynamics with the Indiana Silicon Sphere) [32] was used for collection of the charged particles and free neutrons. The array consisted of 14 concentric rings providing near 4π coverage from 3.6° to 167° in lab. Isotopic resolution was achieved, in the forward angles, for $1 \leq Z \leq 17$ particles and elemental identification was obtained up through the charge of the beam. In the backward angles higher detector thresholds limited particle identification to $1 \leq Z \leq 2$ particles. The entire charged particle array was surrounded by the 4π TAMU Neutron Ball which provided an average event neutron multiplicity. Additional details about the experiment can be found in Refs. [10] and [27].

The experimental events were characterized according to the violence of the collisions through cuts placed on 2-D distributions of the raw neutron and the charge particle multiplicities, as described in Ref. [10]. The cut containing the events with the highest (lowest) neutron and charged particle multiplicities represents the most (least) violent collisions. Five bins (0-4) were created from the 2-D distributions such that each bin would represent a b/b_{max}, or b_{red}, width of 0.2 if one assumed a corresponding triangular impact parameter distribution. Through comparison with molecular dynamics simulations, discussed below, the experimental cuts for bin 2 correspond to a b_{red} selection of ∼0.4 - 0.75. In the following work, the IMF transverse flow is examined for the mid-peripheral collisions (bin 2) from both the experiment and simulations.

The transverse flow is often defined as the slope of the average momentum in the reaction plane, $\langle Px \rangle$, in the midrapidity region [33–35]. Determination of the in-plane momentum requires knowledge of the reaction plane. The azimuthal correlation method [36], in combination with the transverse momentum analysis method [37], was used to reconstruct the reaction plane from the momentum of the charged particles. However, the slope of the midrapidity region could not be accurately extracted for the heavier IMF fragments due to incomplete detection at negative center-of-mass rapidities. Therefore, the flow was quantified by calculating the average in-plane transverse momentum from $0.0 \leq Y_r \leq 0.45$ [38–40], where the reduced rapidity is defined as $Y_r = Y_{cm}/Y_{cm,proj}$. In the following the extracted flow is designated as $\overline{\langle Px \rangle}$. Special attention was taken in accounting for the lack of momentum conservation, due to the reaction plane reconstruction [36, 38], and the anti-correlation that can occur between the heavier fragments and the reaction plane [33] before extracting the $\overline{\langle Px \rangle}$. A more detailed description of these procedures can be found in Ref. [10].

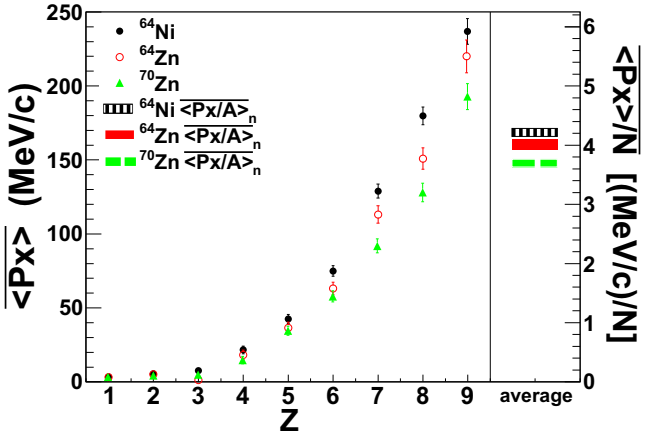

FIG. 1. (color online) Transverse flow, $\overline{\langle Px \rangle}$ (left axis), for Z = 1−9 particles from mid-peripheral collisions in the the ^{70}Zn+^{70}Zn, ^{64}Zn+^{64}Zn, and ^{64}Ni+^{64}Ni collisions (left). The nucleon-averaged flow, $\overline{\langle Px/A \rangle / N}$ (right axis), calculated for each system is presented by the horizontal bars (right).

In Fig. 1 the transverse flow, $\overline{\langle Px \rangle}$, for the Z = 1−9 particles is shown for the mid-peripheral collisions from ^{64}Ni+^{64}Ni, ^{64}Zn+^{64}Zn, and ^{70}Zn+^{70}Zn reactions. In the following discussion the intermediate mass fragments (IMFs) will be defined as all $3 \leq Z \leq 9$ fragments. A clear separation in the flow of the IMFs between the three systems is observed with the ^{64}Ni system exhibiting the largest flow followed by the ^{64}Zn system and then the ^{70}Zn system. In Ref. [10] this was interpreted as a balance between the mass-dependent mechanisms (mean-field and NN-collisions), which would cause the ^{64}Ni and ^{64}Zn systems to have equivalent flow, and the charge-dependent mechanisms (Coulomb repulsion), which would cause the Zn systems to exhibit similar flow.

III. DYNAMICAL MODELS

As mentioned above, the aim of this paper is to examine how the sensitivity of the IMF flow to $E_{sym}(\rho)$

depends on the theoretical description of the reaction dynamics. This is accomplished through a comparison of the antisymmetrized molecular dynamics (AMD) model [28], the constrained molecular dynamics (CoMD) model [29, 30], and the stochastic mean-field (SMF) model [31].

The AMD model [28] with wave packet diffusion and shrinking was used to simulate the dynamics of the reaction up to a time of 300 fm/c, after which the Gemini code [41] was used to statistically de-excite the hot fragments. The practice of using Gemini as an afterburner to AMD has been discussed previously [28, 42]. Since the total wavefunction in AMD is antisymmetrized, the Pauli principle, or the Fermionic nature of the nucleus, is respected at all times. This is computationally expensive limiting the length of the simulation (in this case to 300 fm/c). In the CoMD model [29, 30], the Pauli principle is treated though examination of the occupation density [29, 30] of each nucleon and, therefore, reduces the computational requirements. Thus, the CoMD model was used to simulate the reaction to 3000 fm/c allowing for the majority of the hot fragments to dynamically de-excite. After 3000 fm/c the Gemini code was applied to break-up any unstable or long-lived excited fragments.

In contrast to the molecular dynamics models (AMD and CoMD), the SMF simulation [31] is a mean-field model where each nucleon is represented by 100 test particles which are propagated through a mean-field according to the Boltzmann-Langevin transport equation [40]. The simulation is followed until the time t = 220 fm/c, where primary fragments are formed and well separated. A phase-space coalescence code [43] was applied to the test particle distribution to determine the fragment identities. A statistical decay code, such as Gemini was not applied to the SMF calculation. Previous work has demonstrated that the IMF flow, as predicted by SMF, is only slightly affected by secondary decay, see for instance Ref. [44]. We also verified that the IMF flow did saturate by 220 fm/c, as also expected on the basis of previous studies [40, 45, 46].

The nucleon-nucleon interaction or mean-field potential used in each model was chosen to produce an EoS with a soft compressibility, K, for symmetric nuclear matter between 200-230 MeV. Therefore, the symmetric part of the EoS was kept relatively constant between the models and the isospin-dependent part of the interaction could be varied to examine the sensitivity of the results to the symmetry energy.

The different forms of the symmetry energy can be characterized by their magnitude, slope, and curvature at the saturation density ($\rho_\circ = 0.16 fm^{-3}$). The slope and curvature of the symmetry energy are defined, respectively, as

$$L = 3\rho_\circ \frac{\partial E_{sym}(\rho)}{\partial \rho}|_{\rho_\circ} \qquad (1)$$

TABLE I. Symmetry energy (E_{sym}), slope (L), curvature (K) at normal nuclear density from the different forms of the density dependence of the symmetry energy used in the theoretical simulations.

Simulation	Form	$E_{sym}(\rho_\circ)$	L (MeV)	K_{sym} (MeV)
AMD	Stiff	30.5	65	-96
	Soft	30.5	21	-277
SMF	Stiff	33	95	-72
	Soft	33	19	-249
CoMD	Super-Stiff	30	105	93
	Stiff	30	78	-24
	Soft	30	51	-65

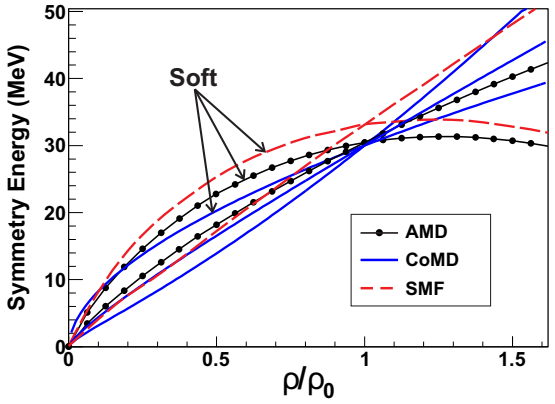

FIG. 2. (color online) The different forms of the density dependence of the symmetry energy used in the AMD, CoMD, and SMF simulations. The soft density dependence is indicated for each calculation. Additional details on the different forms of $E_{sym}(\rho)$ are shown in Table I.

and

$$K_{sym} = 9\rho_\circ^2 \frac{\partial^2 E_{sym}(\rho)}{\partial \rho^2}|_{\rho_\circ}. \qquad (2)$$

In Table I the symmetry energy, slope, and curvature at saturation density for the different parameterizations used in each model are presented. Additionally, the symmetry energy is plotted as a function of the reduced density for each parameterization in Fig. 2. In comparing the different forms of the symmetry energy, it is important to note that the IMF flows should probe density regions near and below $\rho_\circ$ [10]. As shown, the $E_{sym}(\rho_\circ)$ values used in each model are consistent with the current constraints of $30 \lesssim E_{sym}(\rho_\circ) \lesssim 34$ [14]. Thus, the sensitivity of the results to the slope of the symmetry energy, which is much less constrained, can be compared.

The transverse flow for the $Z = 1-9$ fragments calculated from the AMD, CoMD, and SMF models with a stiff form of the symmetry energy is presented in Fig. 3. The trend observed in the experimental data (Fig. 1), which showed increased flow as a function of fragment charge, is reproduced by each simulation. Despite the similarity in the overall trend, the magnitude of the flow and the

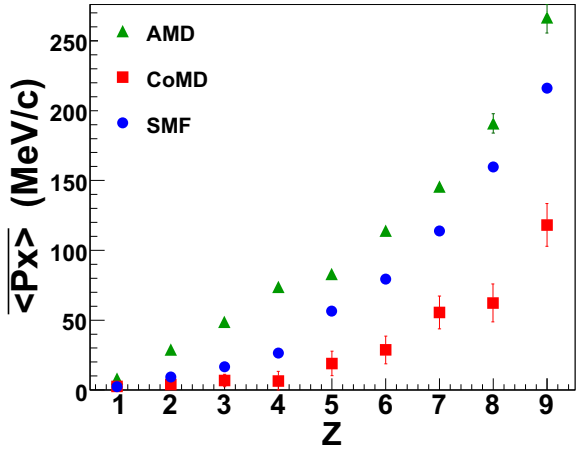

FIG. 3. (color online) Transverse flow, $\overline{\langle Px \rangle}$, as a function of the charge (Z) of the fragments from the AMD, CoMD, and SMF models. The results are presented for the mid-peripheral collisions from the ^{70}Zn+^{70}Zn reaction with the stiff parameterization of the symmetry energy for each model.

progression of the flow for the Z $<$ 5 fragments significantly differs between the models. In the experimental data the flow increases with Z^2. This is best reproduced by the CoMD and SMF models, while the AMD model shows an almost linear increase in the flow with increasing charge. These results present the first indication of the variations that can be observed between the models due to the different treatments of the nuclear dynamics.

Due to the computational requirements of each model, the theoretical results have not be filtered to match the experimental acceptances. When directly comparing the experimental and theoretical results a ratio of the IMF flow between each system is used to minimize the experimental biases by examining only the relative differences in the flow.

IV. COMPARISON OF EXPERIMENT AND THEORY

The relative differences in the IMF flow between each system have been shown to be sensitive to the form of the symmetry energy [10]. To facilitate the comparison between theory and experiment, a nucleon-averaged transverse flow, $\overline{\langle Px \rangle / N}$, was calculated from the flow of the Z = 3−9 fragments. The average in-plane momentum of the Z = 3−9 fragments was calculated as,

$$\frac{\langle Px \rangle}{N} = \left(\sum_{f=0}^{N_f} (Px)_f \right) \div N_n \qquad (3)$$

where N$_f$ (N$_n$) is the total number of fragments (nucleons) in a given rapidity window each with an in-plane momentum of $(Px)_f$. The nucleon-averaged transverse flow was then extracted over the range $0.0 \leq Y_r \leq 0.45$ for each system. The experimental nucleon-averaged flow from each system is shown in right panel of Fig. 1 and represent an average of the IMF flow.

In order to quantitatively compare the difference in the nucleon-averaged flow from system to system the ratio

$$R_{Flow} = \frac{\overline{\langle Px \rangle / N}^{^{64}Zn} - \overline{\langle Px \rangle / N}^{^{70}Zn}}{\overline{\langle Px \rangle / N}^{^{64}Ni} - \overline{\langle Px \rangle / N}^{^{70}Zn}} \qquad (4)$$

was constructed and defines the magnitude of the flow from the ^{64}Zn system in comparison to the ^{64}Ni and ^{70}Zn systems. Thus, when $R_{Flow} = 1$ the flow of the ^{64}Zn system equals that of the ^{64}Ni system and when $R_{Flow} = 0$ the ^{64}Zn and ^{70}Zn systems have equivalent values of flow. As mentioned above, the ratio should minimize any experimental biases and allow for the relative differences in the flow to be compared between the experiment and theory. A value of $R_{Flow} = 0.61 \pm 0.14$ was calculated from the experimental IMF flows for the mid-peripheral reactions as shown in Fig. 1. This represents that the nucleon-averaged flow from ^{64}Zn system was below that of the ^{64}Ni system and above the ^{70}Zn system. The same procedure described above for calculating the R_{Flow} for the experiment was completed for the AMD, CoMD, and SMF models.

In Ref. [10] the AMD, with a stiff form of the symmetry energy, was able to reproduce the experimental R_{Flow} values as a function of the impact parameter. In contrast, the SMF and CoMD models did not show the same impact parameter dependence as AMD, in which the R_{Flow} decreased with increasing impact parameter. However, one should notice that SMF simulations are not well suited to investigate the impact parameter dependence of this observable because, for central collisions in the beam energy range considered here, they underestimate the IMF multiplicity. The CoMD model showed nearly equivalent flow from the Zn systems in the central collisions ($R_{Flow} \cong 0$) and separation between the Zn system in the peripheral collisions ($R_{Flow} > 0$). However, in these central and peripheral collisions the concept of flow is not as clearly defined as in mid-peripheral reactions, where the flow signature is the strongest [45, 47, 48]. Thus, the differences in the fragmentation of the models, as mentioned for the SMF model, could produce significant differences in the flow. While the models differed in the central and peripheral collisions, a consistency was observed in the mid-peripheral collisions. In these reactions the separation in the nucleon-averaged flow between all three systems was present for the AMD, CoMD, and SMF simulations. This offers the opportunity to compare the theoretical results, where they provide a consistent description of the IMF flow, to the experimental data. Specifically, the sensitivity to E$_{sym}(\rho)$ for the nucleon-averaged flow can be examined from the simulated mid-peripheral collisions.

The R_{Flow} values from the different symmetry energy parameterizations of each model are compared to the experimental data in Fig. 4 for the mid-peripheral collisions. As expected from the comparison in Ref. [10], the

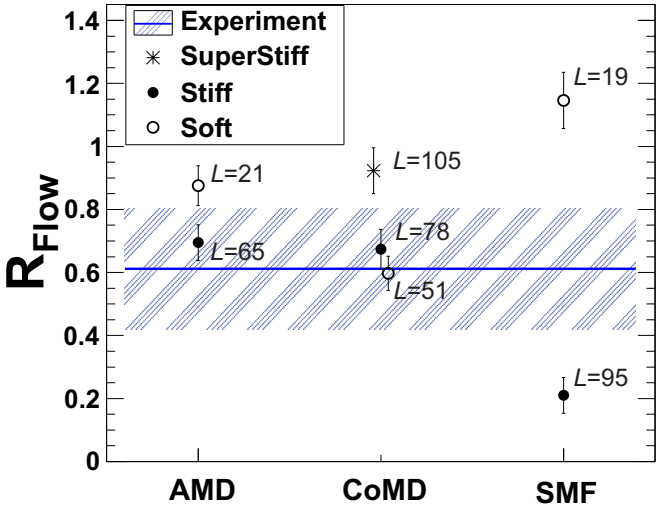

FIG. 4. (color online) R_{Flow} value from the nucleon-averaged flow of the mid-peripheral reactions is shown for the different symmetry energy parameterizations of the AMD, CoMD and SMF models. The corresponding symmetry energy slope (L) is shown next to each calculation. The experimental value is represented by the solid blue line with the statistical uncertainty shown as the hashed blue area.

stiff density dependence of the symmetry energy from the AMD simulation is in good agreement with the experimental results. The soft and stiff CoMD calculations are both in agreement with the experimental R_{Flow} measurement, while the super-stiff CoMD calculation overestimated the R_{Flow} value. The SMF model showed the strongest dependence on the symmetry energy with the stiff (soft) $E_{sym}(\rho)$ producing a smaller (larger) R_{Flow} value then the experiment.

The AMD model shows agreement for a slope of $L = 65$ MeV and demonstrates that a very soft form of the symmetry energy (L = 21 MeV) is unable to reproduce the experimental data. A consistent result is obtained with the CoMD model showing agreement with L = 51 and 78 MeV. The CoMD model also shows that a very stiff form of the symmetry energy (L = 105 MeV) produces a R_{Flow} value larger than the experimental constraints. The results from the SMF model, in agreement with the AMD and CoMD, demonstrate that neither a very soft (L = 19 MeV) or stiff (L = 95 MeV) form of the symmetry energy can reproduce the experimental IMF flow. A linear interpolation between the soft and stiff SMF results indicates that the best agreement with the experimental data would result from a slope of 62 MeV. Despite the differences in the theoretical models, the relative agreement in the form of the symmetry energy that reproduces the experimental data is surprising.

In the examined energy region, 35 MeV/nucleon, the maximum density achieved in the reaction is likely around 1.5 $\rho/\rho_\circ$ and the mid-rapidity IMFs have been suggested to originate from a low density neck region, as suggested by previous AMD and SMF studies [42, 49, 50]. According to these models, the results discussed above, which suggest that the slope of the symmetry energy should be in the range of ∼50 - 80 MeV, probe a density region near and below the saturation density.

Indeed, in the SMF model the difference between the two calculations can be connected to the low density behavior of the symmetry energy. According to the higher value of the symmetry energy below saturation density, the soft interaction will decrease the attractive mean-field potential for the neutron rich systems, more than in the stiff case. Therefore, the mean-field will be less attractive for the ^{64}Ni system (N/Z = 1.33), with respect to the ^{64}Zn system (N/Z = 1.13). This should produce a larger decrease in the ^{64}Ni IMF flow in comparison to the ^{64}Zn IMF flow for a soft $E_{sym}(\rho)$. The soft SMF results showed this effect with the ^{64}Zn system exhibiting a larger IMF flow than the ^{64}Ni system, producing a $R_{Flow} > 1$. In the case of the stiff symmetry potential, which is less repulsive, Coulomb effects dominate and one observes that the ^{64}Ni IMF flow is larger than the ^{64}Zn IMF flow in the SMF model producing R_{Flow} near 0.25. The same trend is seen also in AMD calculations, though the results corresponding to the two different $E_{sym}(\rho)$ are much closer. This can be attributed to the fact that, as reported in Table I, the soft and stiff interactions used in AMD have closer L values, with respect to the parametrizations used in SMF. Moreover, it is also expected that in SMF lower density regions are explored, where soft and stiff parametrizations diverge, while they are obviously rather close in the proximity of the normal density.

The opposite trend in the relationship between L and R_{Flow} observed in the CoMD model may suggest that, due to the different model ingredients, the IMF flow results are sensitive to a different density domain. In fact, if the IMF flow from the CoMD model is originating from a region above the saturation density, as expected on the basis of the fast fragmentation dynamics predicted by the model, then the isospin-dependent part of the interaction would have the opposite effect relative to the low-density region, thus, explaining the difference in the observed trend in comparison to AMD and SMF results.

It is interesting to notice that, in spite of the different reaction dynamics in the three models considered; the R_{flow} observable appears to be suitable to pin down a sensitivity to the symmetry energy. All models lead to similar conclusions about the L value that better reproduce the experimental data, independent of the reaction mechanism.

V. CONCLUSIONS

In conclusion, the transverse flow of intermediate mass fragments has been investigated for mid-peripheral reactions in the 35 MeV/nucleon ^{70}Zn+^{70}Zn, ^{64}Zn+^{64}Zn, and ^{64}Ni+^{64}Ni systems. The AMD, CoMD, and SMF models were compared with the experimental data in or-

der to examine how the treatment of the nuclear dynamics can affect the sensitivity of the model to the nEoS. The results demonstrated that the relative differences in the IMF transverse flow is dependent on the isospin-dependent part of the mean-field or nucleon-nucleon interaction in each model. However, the sensitivity of the IMF flow to the form of the symmetry energy varied between the different simulations. For example, the SMF model showed the largest correlation between the R_{Flow} observable and the slope (L) of the symmetry energy.

Despite the differences in the models, better agreement with the experimental data was achieved with a form of the symmetry energy having a slope (L) in the range of ∼50-80 MeV for each simulation, which is in good agreement with current constraints [14, 51]. However, the significance of this agreement is outweighed by the differences in the overall sensitivity of the models to L. Overall, the results indicate that robust constraints on the density dependence of the symmetry energy will require consistent theoretical comparisons. Additionally, the use of multiple models, while time-consuming, should become an important aspect in trying to extract information on the form of the nEoS from heavy-ion collision observables.

VI. ACKNOWLEDGEMENTS

We would like to thank the staff members of the Texas A&M Cyclotron Institute for the excellent beam quality. This work was supported in part by the Robert A. Welch Foundation through grant No. A-1266, and the Department of Energy through grant No. DE-FG03-93ER40773. We would further like to thank Dr. A. Ono for use of the AMD code, Dr. M. Papa for use of the CoMD code, and Dr. R. J. Charity for use of the Gemini code. We would also like to thank the Laboratory for Molecular Simulation at Texas A&M University and the Texas A&M Chemistry Supercomputer funded by the National Science Foundation Grant No. CHE-0541587.

[1] A. W. Steiner, M. Prakash, J. M. Lattimer, and P. J. Ellis, Phys. Rep. **411**, 325 (2005).
[2] J. M. Lattimer and M. Prakash, Science **304**, 536 (2004).
[3] J. R. Stone, J. C. Miller, R. Koncewicz, P. D. Stevenson, and M. R. Strayer, Phys. Rev. C **68**, 034324 (2003).
[4] B. A. Li and A. W. Steiner, Phys. Lett. B **642**, 436 (2006).
[5] B. A. Li, Phys. Rev. Lett. **88**, 192701 (2002).
[6] B. A. Li, Nucl. Phys. **A708**, 365 (2002).
[7] V. Baran, M. Colonna, V. Greco, and M. Di Toro, Phys. Rep. **410**, 335 (2005).
[8] B. A. Li, L. W. Chen, and C. M. Ko, Phys. Rep. **464**, 113 (2008).
[9] D. V. Shetty, S. J. Yennello, and G. A. Souliotis, Phys. Rev. C **76**, 024606 (2007).
[10] Z. Kohley, L. W. May, S. Wuenschel, A. Bonasera, K. Hagel, R. Tripathi, R. Wada, G. A. Souliotis, D. V. Shetty, S. Galanopoulos, M. Mehlman, W. B. Smith, S. N. Soisson, B. C. Stein, and S. J. Yennello, Phys. Rev. C **82**, 064601 (2010).
[11] M. A. Famiano, T. Liu, W. G. Lynch, M. Mocko, A. M. Rogers, M. B. Tsang, M. S. Wallace, R. J. Charity, S. Komarov, D. G. Sarantites, L. G. Sobotka, and G. Verde, Phys. Rev. Lett. **97**, 052701 (2006).
[12] T. X. Liu, W. G. Lynch, M. B. Tsang, X. D. Liu, R. Shomin, W. P. Tan, G. Verde, A. Wagner, H. F. Xi, H. S. Xu, B. Davin, Y. Larochelle, R. T. de Souza, R. J. Charity, and L. G. Sobotka, Phys. Rev. C **76**, 034603 (2007).
[13] M. B. Tsang, T. X. Liu, L. Shi, P. Danielewicz, C. K. Gelbke, X. D. Liu, W. G. Lynch, W. P. Tan, G. Verde, A. Wagner, H. S. Xu, W. A. Friedman, L. Beaulieu, B. Davin, R. T. de Souza, Y. Larochelle, T. Lefort, R. Yanez, V. E. Viola, R. J. Charity, and L. G. Sobotka, Phys. Rev. Lett. **92**, 062701 (2004).
[14] M. B. Tsang, Y. Zhang, P. Danielewicz, M. Famiano, Z. Li, W. G. Lynch, and A. W. Steiner, Phys. Rev. Lett. **102**, 122701 (2009).
[15] A. Ono and J. Randrup, Eur. Phys. J. A **30**, 109 (2006).
[16] J. Rizzo, M. Colonna, and A. Ono, Phys. Rev. C **76**, 024611 (2007).
[17] M. Colonna, A. Ono, and J. Rizzo, Phys. Rev. C **82**, 054613 (2010).
[18] Y. Zhang, D. D. S. Coupland, P. Danielewicz, Z. Li, H. Liu, F. Lu, W. G. Lynch, and M. B. Tsang, Phys. Rev. C **85**, 024602 (2012).
[19] D. D. S. Coupland, W. G. Lynch, M. B. Tsang, P. Danielewicz, and Y. Zhang, Phys. Rev. C **84**, 054603 (2011).
[20] Z. Xiao, B. A. Li, L. W. Chen, G. C. Yong, and M. Zhang, Phys. Rev. Lett. **102**, 062502 (2009).
[21] Z. Q. Feng and G. M. Jin, Phys. Lett. B **683**, 140 (2010).
[22] Y. Zhang, P. Danielewicz, M. Famiano, Z. Li, W. G. Lynch, and M. B. Tsang, Phys. Lett. B **664**, 145 (2008).
[23] M. Di Toro, S. J. Yennello, and B. A. Li, Eur. Phys. J. A **30**, 153 (2006).
[24] B. A. Li, C. M. Ko, and W. Bauer, Int. J. Mod. Phys. **E7**, 147 (1998).
[25] L. Scalone, M. Colonna, and M. Di Toro, Phys. Lett. B **461**, 9 (1999).
[26] P. Russotto, P. Z. Wu, M. Zoric, M. Chartier, Y. Leifels, R. C. Lemmon, Q. Li, J. Lukasik, A. Pagano, P. Pawlowski, and W. Trautmann, Phys. Lett. B **697**, 471 (2011).
[27] Z. Kohley, L. W. May, S. Wuenschel, M. Colonna, M. DiToro, M. Zielinska-Pfabe, K. Hagel, R. Tripathi, A. Bonasera, G. A. Souliotis, D. V. Shetty, S. Galanopoulos, M. Mehlman, W. B. Smith, S. N. Soisson, B. C. Stein, and S. J. Yennello, Phys. Rev. C **83**, 044601 (2011).
[28] A. Ono and H. Horiuchi, Prog. Part. Nucl. Phys. **53**, 501 (2004).
[29] M. Papa, G. Giuliani, and A. Bonasera, J. Comput. Phys. **208**, 403 (2005).

[30] M. Papa, T. Maruyama, and A. Bonasera, Phys. Rev. C **64**, 024612 (2001).
[31] J. Rizzo, M. Colonna, M. Di Toro, and V. Greco, Nucl. Phys. **A732**, 202 (2004).
[32] S. Wuenschel, K. Hagel, R. Wada, J. Natowitz, S. J. Yennello, Z. Kohley, C. Bottosso, L. W. May, W. B. Smith, D. V. Shetty, B. C. Stein, S. N. Soisson, and G. Prete, Nucl. Instrum. Methods Phys. Res. A **604**, 578 (2009).
[33] D. Cussol *et al.*, Phys. Rev. C **65**, 44604 (2002).
[34] W. Reisdorf and H. G. Ritter, Annu. Rev. Nucl. Part. Sci. **47**, 663 (1997).
[35] S. Das Gupta and G. D. Westfall, Physics Today **46**, 34 (1993).
[36] W. K. Wilson, R. Lacey, C. A. Ogilvie, and G. D. Westfall, Phys. Rev. C **45**, 738 (1992).
[37] P. Danielewicz and G. Odyniec, Phys. Lett. B **157**, 146 (1985).
[38] C. A. Ogilvie *et al.*, Phys. Rev. C **40**, 2592 (1989).
[39] A. Ono and H. Horiuchi, Phys. Rev. C **51**, 299 (1995).
[40] A. Bonasera, F. Gulminelli, and J. Molitoris, Phys. Rep. **243**, 1 (1994).
[41] R. J. Charity *et al.*, Nucl. Phys. **A483**, 371 (1988).
[42] R. Wada, T. Keutgen, K. Hagel, Y. G. Ma, J. Wang, M. Murray, L. Qin, P. Smith, J. B. Natowitz, R. Alfarro, J. Cibor, M. Cinausero, Y. El Masri, D. Fabris, E. Fioretto, A. Keksis, S. Kowalski, M. Lunardon, A. Makeev, N. Marie, E. Martin, Z. Majka, A. Martinez-Davalos, A. Menchaca-Rocha, G. Nebbia, G. Prete, V. Rizzi, A. Ruangma, D. V. Shetty, G. Souliotis, P. Staszel, M. Veselsky, G. Viesti, E. M. Winchester, S. J. Yennello, W. Zipper, and A. Ono, Phys. Rev. C **69**, 044610 (2004).
[43] E. Santini, T. Gaitanos, M. Colonna, and M. Di Toro, Nucl. Phys. **A756**, 468 (2005).
[44] J. D. Frankland *et al.*, Nucl. Phys. A **689**, 940 (2001).
[45] A. D. Sood and R. K. Puri, Phys. Rev. C **69**, 054612 (2004).
[46] R. Nebauer and J. Aichelin, Nucl. Phys. **A650**, 65 (1999).
[47] R. Pak *et al.*, Phys. Rev. C **53**, 1469 (1996).
[48] G. D. Westfall, Nucl. Phys. **A630**, 27 (1998).
[49] B. A. Li and L. W. Chen, Phys. Rev. C **72**, 064611 (2005).
[50] M. Di Toro, A. Olmi, and R. Roy, Eur. Phys. J. A **30**, 65 (2006).
[51] L. W. Chen, C. M. Ko, B. A. Li, and J. Xu, Phys. Rev. C **82**, 024321 (2010).